IEEE Access
Multidisciplinary | Rapid Review | Open Access Journal

Received January 29, 2021, accepted February 7, 2021, date of publication February 22, 2021, date of current version March 4, 2021.

Digital Object Identifier 10.1109/ACCESS.2021.3061102

An Approach for Shadow Detection in Aerial Images Based on Multi-Channel Statistics

GILBERTO ALVARADO-ROBLES, ROQUE A. OSORNIO-RÍOS, (Member, IEEE), FRANCISCO J. SOLÍS-MUÑOZ, AND LUIS ALBERTO MORALES-HERNÁNDEZ, (Member, IEEE)

Department of Mecatrónica, Facultad de Ingeniería, Universidad Autónoma de Querétaro, Campus San Juan del Rio, Queretaro 76807, Mexico

Corresponding author: Luis Alberto Morales-Hernández (lamorales@hspdigital.org)

This work was partially funded by CONACyT Scholarship under Grant 575938 and Grant 783317.

ABSTRACT Shadows are likely to cause flaws in color interpretation, loss of image information or deformation of objects; this is a relevant issue owing to the fact that with the development of unmanned aerial vehicles and satellite devices, object detection by aerial images has become an essential aim to research works. The main contribution of this article is the development of an algorithm that processes shadow detection by detaching the channels red, green, blue and an additional low saturation channel on individual masks; having created those masks, the task of shadow detection is accomplished by conducting a pixel-by-pixel basis with the aid of a decision tree and statistical descriptors extracted out of the image, where the low saturation channel information leads to improvements on shadow detection accuracy in regions that contain asphalt and concrete. Thus, experimental results show the good behavior of shadow detection algorithm in terms of accuracy, over-segmentation, and under-segmentation, in which the accuracy of obtained shadow detection approaches a 94%.

INDEX TERMS Unmanned aerial vehicles, color, remote sensing, image processing, image segmentation, pattern recognition, shadow detection, HSV color space.

I. INTRODUCTION

Aerial image analysis is a research field which has aimed at a thorough, growing trend over the past few years due to the wide range of applications. Accordingly, acquisition systems for taking aerial images were made up by means of a satellite capturing device, which took samples from a considerable distance [1], requiring the use of a high-resolution custom-made camera. The general public was conditioned by the supplier of this service, obtaining these shots at a slow update rate, mainly due to the resources needed by the provider to handle such high resolution images and the high impact image stitching processing time associated to these [2]. Nevertheless, over the past decade, the outbreak of unmanned aerial vehicles (UAV) has been witnessed [3], providing an economically feasible alternative for the average population to take on demand aerial images. This support technology along with the current computing power enables the development of image analysis solutions to be updated under a low cost scheme [4]. Remote sensing solutions based on aerial imaging are extensible to the use of UAV, where a wide range of applications such as the analysis of urban regions, the analysis of forestry areas [5], the optimization of precision agriculture [6], the study of geosciences [7] and the segmentation of urban zones [8] have been developed. Despite the fact that the use of aerial images has increased, there are several factors that hinder the extraction of information, one of which being shadows. Shadows represent one of the main causes of misclassification errors when extracting information from a surface during remote sensing [9]. Images taken in urban areas are assumed to contain many elements capable of causing the appearance of shadows, such as buildings, trees, towers, poles and antennas; Shaded regions diminish the quality of remote sensing, leading to difficulties in subsequent processing and analysis processes [10]. Shadow detection research works have been applied widely for remote sensing applications [11]–[14]. The sensors with higher spatial resolution present a useful tool for aerial imagery. Yet, the consideration of shadows caused by the geometry of the scene has become increasingly important for scenes in urban environments [15].

As previously mentioned, aerial imaging is an important study field in image processing; with the fast development of UAV and satellites, object detection for aerial images has

The associate editor coordinating the review of this manuscript and approving it for publication was Jon Atli Benediktsson.

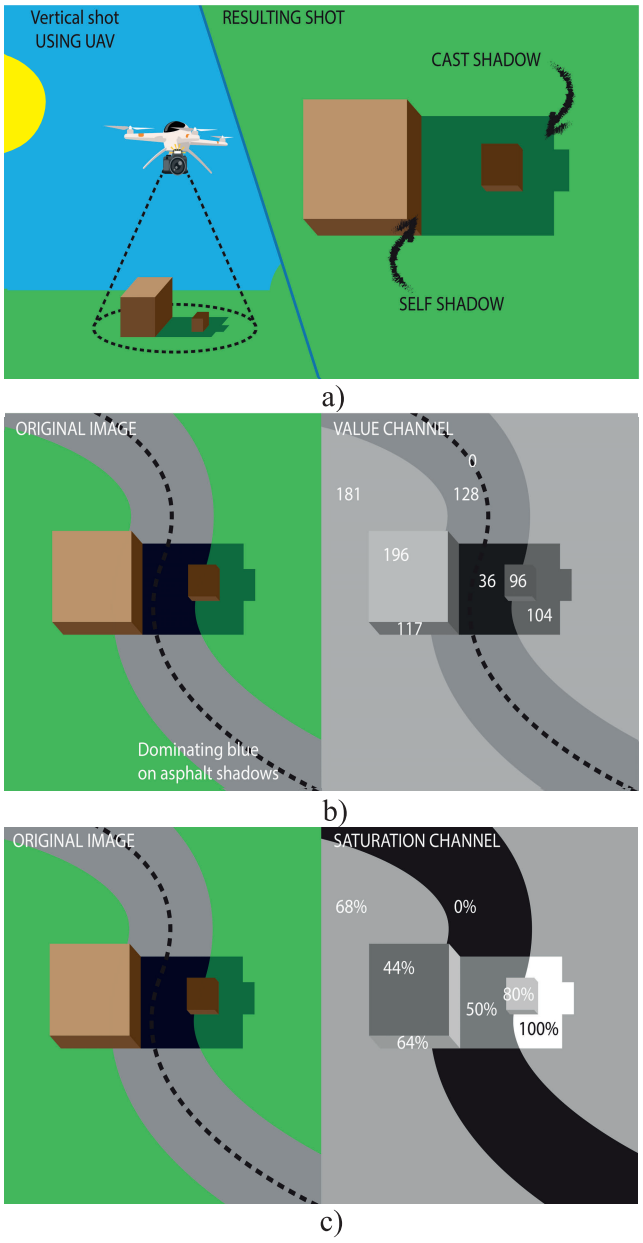

FIGURE 1. Synthetic images, a) UAV image capturing process detail (left) where cast shadow and self shadow are present (right), b) V channel changes under illuminated and shadowed regions, c) S channel changes under illuminated and shadowed regions and the achromatic characteristics in asphalt.

become an interesting topic present in recent research works. Despite the fact that in the latter years significant progress in object detection has been witnessed [16], detection accuracy for aerial images is still improvable due to several conditions; in color aerial images two of the most common factors that diminish accuracy are self-shadows and cast shadows (refer to Fig. 1 (a)). The aforementioned types of shadows could incur issues such as a false color interpretation, a loss of image information or a deformation of objects, impacting negatively on image processing algorithms accuracy.

Shadow detection is a task that could be accomplished by using two principal means. The first approach is based on the use of a background picture to detect shadows in motion images; this solution has been widely studied, where, in the literature, this procedure has been applied mainly for video surveillance applications [17]–[20]. As a second approach, single image processing methods have been published, addressing the issue of shadow detection without the need of background images [21]–[23].

Single image shadow detection methods have many applications in the field of aerial pictures on account of the fact that, for this kind of images, there are no reference images, where the system only has knowledge of the current state of the objective scenario. This kind of methods could be classified into three main categories, which are described next.

The techniques regarding the first category are usually called hard shadow detection. Hard shadow detection algorithms are based on a binary image segmentation process, where a search for the optimal threshold over some image transformation that maximizes shadow area detection is conducted. The methods proposed under this first category are mostly based upon the proposal presented by Tsai [24], whose method builds up a shadow mask by applying a smoothed Otsu threshold onto the image transformation resulting from computing the ratio between the luminance and the hue channels. As an example of a variant based on the method previously quoted, Silva *et al.* [25] proposes the use of the CIELCh color space channels to improve this process.

At a second category, techniques based on the stochastic analysis of the image are present, the method proposed by Mo *et al.* [26] shows how this task is carried out by generating a shadow detection probabilistic map under a Gaussian mixture model (GMM) [27].

Finally, the third category is established by the methods that use clustering techniques for detecting shadows by image segmentation. These methods use luminance characteristics in order to binarize the image, as a case of this variant, the work by Usha Nandini and Leni [28] proposes an image segmentation based on regions particle swarm optimization (PSO) and K-means clustering segmentation using hue-saturation-value (HSV) color space.

According to the literature reviewed, shadow detection approaches tend to focus on distinguishing shadowed and non-shadowed regions, applying a threshold over the result and a last filtering step over it. The great majority of studies have only focused on the processing of either satellite images or UAV images. Published researches fail to provide a versatile solution, mainly due to the divergent color histograms at pictures acquired by the aerial image acquisition methods cited before. In the reviewed literature, cast shadows and self shadows present certain characteristics in terms of luminance and hue, and although those features are helpful in the shadow detection process, there are some parameters and characteristics of the scene that could present an obstacle when executing the shadow segmentation task. On this

regard, as it could be observed in Fig. 1 (a), different light conditions produced by the light source rays occlusion result in changes in the captured colors. These chromatic characteristics changes are noticeable at the S and V channels, which are shown at Fig. 1 (b) and (c) respectively, where asphalt and concrete regions tend to present a quite different value compared to the rest of the image areas considered in urban zones. For the case of the S channel, the values of illuminated regions are close to zero in contrast with the shadow regions, where values are significantly higher. Contrarily, when analyzing the V channel, there not seems to be any perceptible value divergence between regions; this could result in a region misclassification during statistical analysis in any urban zone image, caused by the achromatic color characteristics of asphalt and concrete present in aerial imaging. In addition to this, the specific conditions of the image acquisition processes within the methods reviewed require a large image contrast to detect the shadowed regions accurately, decreasing the range of these methods applications; even more, the filtering process attached to the reviewed methods could lead to a boundary misshaping error at detected shadows.

In the present work, an innovative method to segment cast shadows and self-shadows in aerial images captured in urban regions is stated; the purpose of this approach is to improve the accuracy of shadow detection results in UAV captured images; moreover, the proposed method is ambivalent, as it is also suitable for processing satellite captured images as well; the proposed algorithm is based on HSV color space and aims to tackle the disadvantages mentioned before, such as the discussed asphalt and concrete region misclassification. The proposed method could be applied by following the following steps. The first step of the process is the creation of masks related to the maximum color components red (R), green (G), blue (B) and, added to these, an additional low saturation (LS) mask is created as well; as a second step, taking into account the masks created before, a statistical analysis over the value (V) channel is undertaken, a factor is calculated on a process of standardization, allowing the application of the proposed method under different scenarios, such as urban zones with vegetation, asphalt, concrete and buildings; the third and final step is based in an automated shadow segmentation, which is completed by the use of a decision tree. Consequently, according to the literature revision, this work presents a series of contributions that aim to offer a solution to the drawbacks found, those contributions are discussed next. As a first contribution, the proposed approach for shadow detection presents as a novelty the use of a threshold for the saturation channel, empowering its application at urban images, where asphalt and concrete sections show unusual chromatic characteristics. Even more, this approach benefits from presenting a compact yet efficient image processing algorithm, basing itself on the use of decision trees and basic statistical measurements in a pixel-by-pixel independent fashion, what could lead to fast parallel processing implementations. In addition, splitting the analyzed image into its RGB channels allows the specific hyper-parameter tuning process for each decision tree branch and in consequence results in a more accurate and specific process. Furthermore, the proposed method contributes to this research area offering an adaptive solution able to perform shadow segmentation with either satellite and UAV captured images. The methodology presented in this work was tested and compared to other four recently published methodologies that deal with UAV or satellite imagery, taking into account the accuracy of the different shadow detection algorithms in terms of accuracy, over-segmentation, and under-segmentation, where the proposed methodology showed appreciable improvements in the results obtained as against the other two methodologies.

II. RELATED WORK

Shadows constitute a difficulty at object detection and segmentation algorithms, where these kind of features are prone to cause misshaping errors for objects contours. Image segmentation for object extraction is a recurrent research issue, it is a field in which the semi-supervised learning techniques have demonstrated their effectiveness, specifically for region segmentation techniques, also known as salient objects detection [29], [30]; in order to reduce the work needed for generating image masks manually, unsupervised segmentation methods for outdoor images have been presented recently, as well [31], [32]. Nevertheless, shadows present a drawback for the accuracy of such algorithms, since shadows alter the perceived shape of objects as mentioned before.

A considerable number of frameworks addressing the shadow detection issue by using a single image have been published. Single image shadow detection methods have many applications in the field of outdoor pictures owing to the fact that for this kind of images, background reference images and previous state frames are not always present, having a system fed by only the current state. A noteworthy proposal for tackling the previously described problem was presented by Tsai [24]. In his work, a method which builds up a shadow mask is developed, basing its functionality on applying a smoothed Otsu threshold onto the image transformation resulting from computing the ratio between the luminance and the hue channels.

As a consequence of Tsai *et al.* work, a variant based on this proposal is presented by Tian *et al.* [33]. The kernel of their implementation contains spectrum ratio computation, sRGB color space and it is complemented with an edge detection to perform the shadow detection at outdoor scenarios.

With the goal of improving shadow detection results, a methodology by Silva *et al.* [25] is proposed. In their scheme, the main contribution in color analysis is the proposal of the Conversion from CIELab color space to its polar representation CIELCh. This is performed and achieved to use the hue channel in order to profit the fact that shadows have larger hue values, and define the specthem ratio by relating the hue and the luminance parameters.

The methodologies based on artificial neural networks structures have been widely adopted at image processing tasks. For shadow detection it is worth to mention the

proposal presented by Hosseinzadeh *et al.* [34]. At their work, they present an approach for shadow detection based on a Convolutional Neural Network (CNN) in which the over-segmentation is minimized during the training proposed by the author, although the CNN could automatically learn features from the input images, a prior hyper-parameter tuning is needed and ground truth data sets are needed. There are some structural hyper-parameters that affect the performance of shadow detection algorithms, such as the number and input sizes for the convolutional layers, the learning rate, and the maximum number of training iterations; which could lead to deficiencies at evaluating certain images by this method.

Continuing on this line, there exists a group of methods composed by the algorithms that perform the shadow detection task with the aid of a color space transformation, transforming the RGB channels to the CIELab Color space. This particular conversion (RGB to CIELab) is carried out by Suny and Mithila [35], where the luminance channel information is used for segmentation, compensating the lightness of shadowed regions for developing a shadow removal process.

Finally, the methods that use luminance features to binarize the image are worth considering, as in the case of this variant, the work presented by Usha Nandini and Leni [28] proposes a segmentation of images based on regions using an algorithm based on the PSO and the K-means clustering algorithms. This segmentation is achieved through the use of the HSV color space in conjunction with a prior bilateral filtering process to reduce noise in the image. Such methodology shows a loss of accuracy when the image shows a large contrast at chromaticity values.

According to the consulted literature sources, shadow detection algorithms tend to distinguish shaded and unshaded regions by using different color characteristics in the image and shadow properties, and after that, applying a threshold on the result, ending up with a filtering step. Many studies focus on the classification of shadows according to image characteristics such as the mentioned chromaticity and luminance; however, these characteristics have limitations based on the scene conditions or the image capturing device used. Therefore, it would be desirable to have a shadow detection method that could adapt itself for being used for a wider range of scenes and pictures without additional parameters or threshold modifications.

III. METHODOLOGY

The proposal was tested against UAV and satellite imagery. On the UAV experiments, urban regions shots were taken by a setup consisting of a drone device (DJI Phantom 4) with a 12.4MP camera, a variable flight altitude was set for each image in order for the shot to contain enough information and maintaining a good ground resolution. On the satellite experiments, images were obtained from the wide-area motion imagery (WAMI) system in Porto Alegre (Brazil) and the Airbus SPOT-6 satellite. The criteria in the development of the proposed approach is given by the characteristics of the shadows mentioned by [25], where the key features that could be found in shadows are:

- Low luminance (intensity), because the electromagnetic radiation from the sun is blocked in these regions [33].
- High saturation with short blue-violet wavelength, mostly due to the Rayleigh effect of atmospheric scattering [36].
- Increased hue values, because of the intensity variations at shaded areas, which correspond to color spectrum wavelength values [37].

Taking into account the features in shadows, the proposed method aims to improve the shadow detection by performing an statistical pixel-by-pixel analysis of the V channel by creating masks of color components prevalence for R, G and B channels; added to these, the proposed method adds an additional LS mask. The proposed methodology for shadow detection is shown in Fig. 2, where the main process is divided into three main steps, named as masks creation, classification, and result.

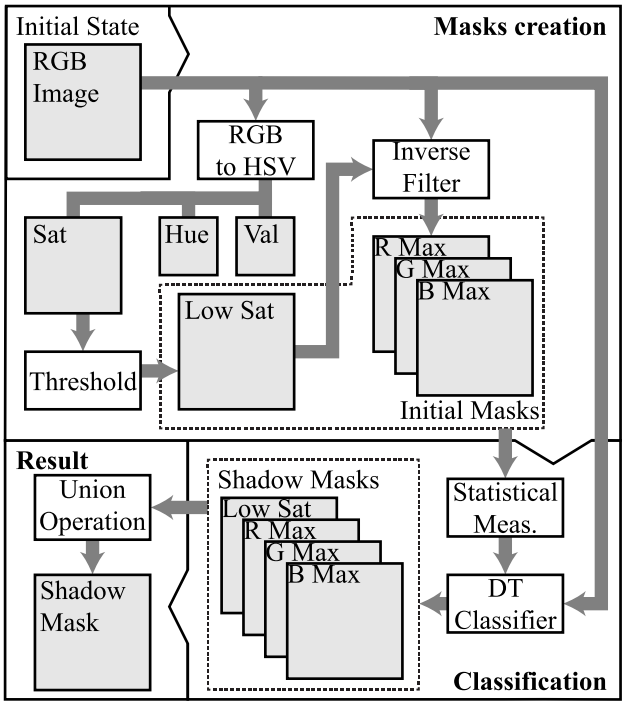

FIGURE 2. Proposed methodology for shadow detection, each matrix is represented with a gray filled block.

The results obtained during the execution of the proposed methodology described in Fig. 2 are displayed in Fig. 3, where the statistical analysis required to complete shadow detection is presented at the classification step, producing distinct shadow masks which are finally joined into a unique shadow detection binary mask.

Mask creation: The first step of the process is based on the transformation of the input image (i) into HSV color space; the separation of channels is carried out by using saturation channel values, where the definition of this criterion is

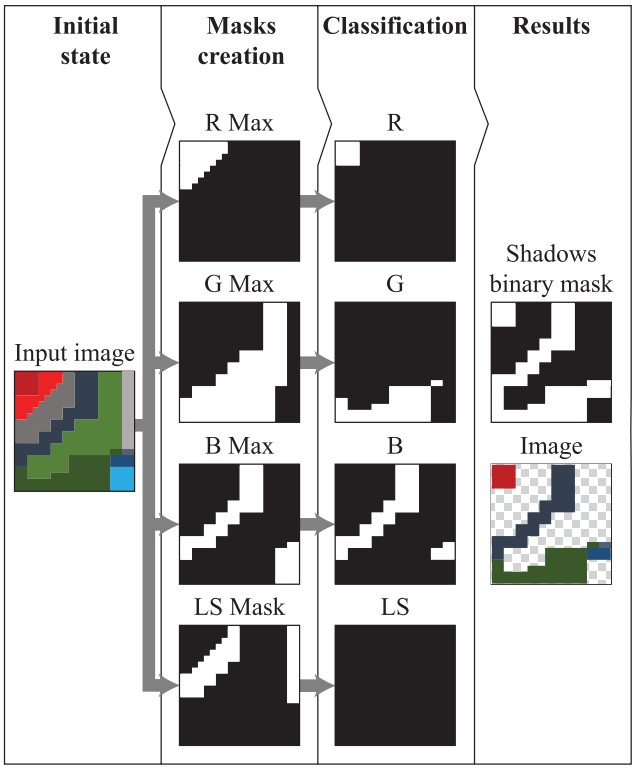

FIGURE 3. Shadow detection outputs scheme.

established according to a reference value range, where for the proposed method, the range determined for LS pixels is set out by the condition $S < 0.1$; in this first thresholding step, an image (M_{LS}) is obtained. The pixels of M^c_{LS} are used to extract the masks M_R (dominating red channel mask), M_G (dominating green channel mask), and M_B (dominating blue channel mask), according to the criteria shown in (1), where dominating color masks are created for each color channel.

$$M_R(x,y) = \begin{cases} 1, & \text{if } R = \arg\max_c M^c_{LS}(x,y) \\ 0, & \text{otherwise} \end{cases}$$
$$M_G(x,y) = \begin{cases} 1, & \text{if } G = \arg\max_c M^c_{LS}(x,y) \\ 0, & \text{otherwise} \end{cases}$$
$$M_B(x,y) = \begin{cases} 1, & \text{if } B = \arg\max_c M^c_{LS}(x,y) \\ 0, & \text{otherwise} \end{cases} \quad (1)$$

According to (1), if the non-zero mask values are replaced by the RGB values the separation proposed can be observed as is shown in Fig. 4 where each image containing particular information related to the analyzed channel can be discerned, it is mainly noticeable that Fig. 4 (d) contains most of the shadows in concrete and asphalt zones, this is due to the Rayleigh effect that is more evident in the regions mentioned before. In addition, it can be observed in Fig. 4 (e), that the proposed method realizes the separation of low saturation colors that includes all pixels with such characteristics.

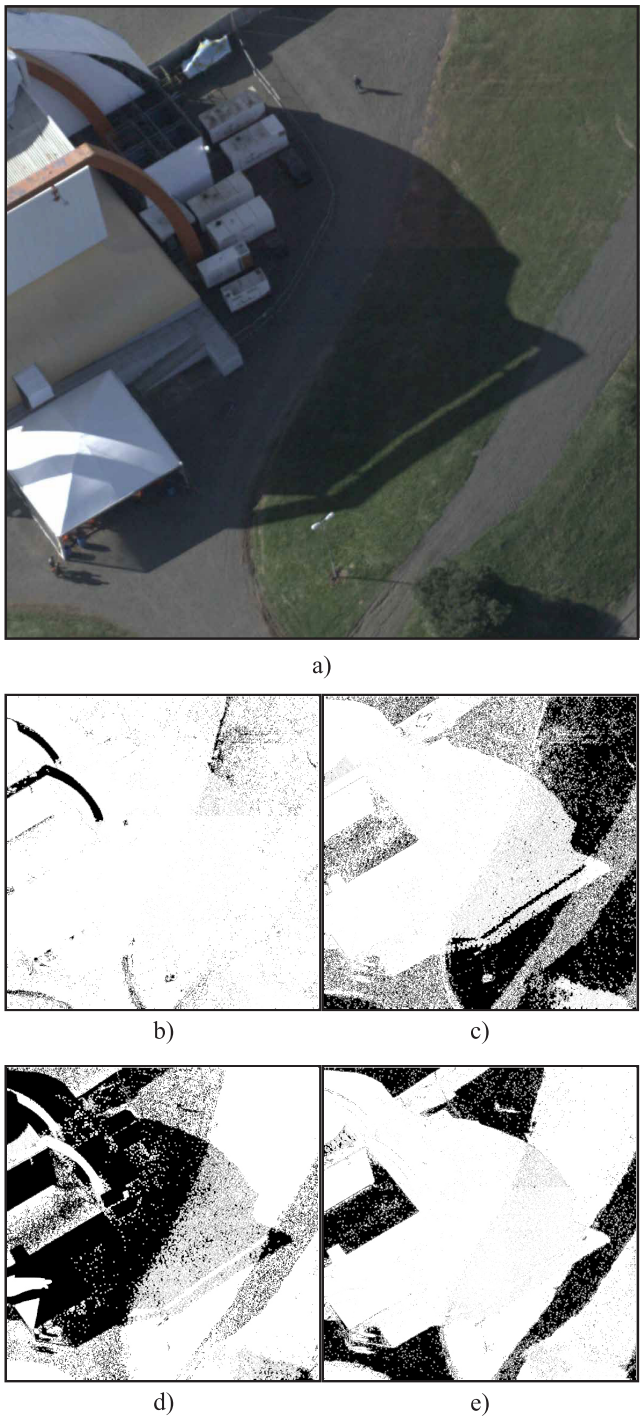

FIGURE 4. Proposed color features separation. (a) Input image, (b) R channel mask, (c) G channel mask, (d) B channel mask, and (e) LS channel mask.

Classification: Using the binary masks content obtained from (1) as condition, the V channel statistics are computed individually for R, G, and B channels in i, where the method computes statistics such as the mean ($\overline{x}$), the standard deviation (S) and the skewness (κ). The channel separation based on the masks (R, G, B) and the addition of LS mask

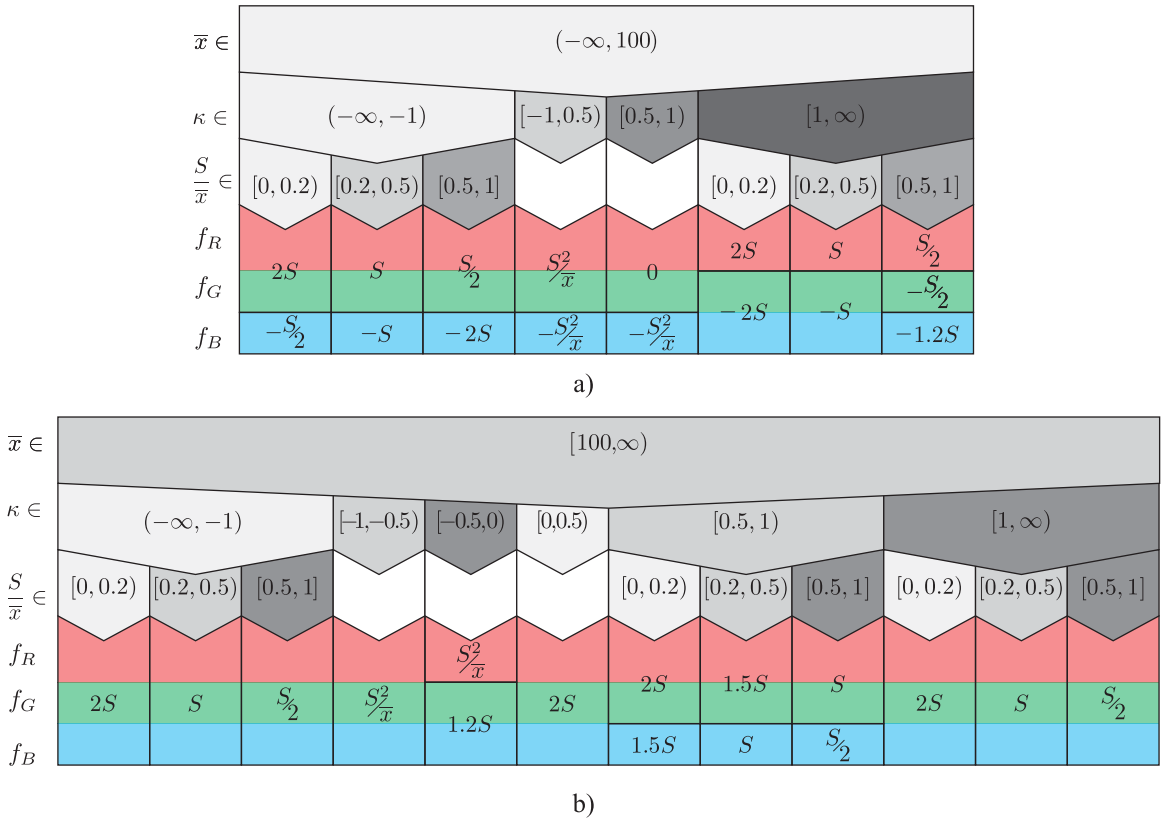

FIGURE 5. Vertical decision tree block structure for channel factors f_R, f_G and f_B for lower (a) and upper (b) values of $\overline{x}$.

in conjunction allow a pixel-by-pixel approach for shadow detection; the proposed method uses the statistical distribution of colors present in each channel as the colors depict different chromaticity characteristics under sunlight and shadow conditions, the statistics are more accurate when such color features are measured individually.

Therefore, the proposed method has different parameters for each channel; the main parameters are the statistical measures for each dominating color channel mask; specifically the mean ($\overline{x}$), the standard deviation (S), and the skewness (κ); the most relevant parameter is $\overline{x}$ since it establishes the starting point to accomplish the shadow detection. Meanwhile, S establishes the dispersion of color information into the image, that is why it is a reference parameter for establishing the real presence of shadows in the analyzed channel. Finally, the third parameter, κ, is useful to locate the asymmetry in color distribution. The mentioned parameters are used in each reference mask in different manners in every shadow detection; the fundamental operations for completing the shadow detection process are presented in (2).

$$d_b = \begin{cases} 0, & \text{if } V > (\overline{x} - f) \\ 1, & \text{otherwise} \end{cases} \tag{2}$$

where $\overline{x}$ is the mean of V in each channel; V is the value in the analyzed channel mask, and f is the adjustment parameter for shadow detection, which is defined according to the statistical values previously stated. In the case of the LS mask the criteria is defined by specific conditions that are shown in (3), this criterion is based on the color characteristics that concrete and asphalt regions acquire under sunlight conditions, where these areas are the mainly represented in the LS mask, in which it can be observed that the range of values to perform the shadow detection is defined from 5 to 15. This value is set for discarding the lowest values that belong to regions with near-black colors, these regions do not contain enough color information that could be useful for further processing.

$$d_b = \begin{cases} 0, & \text{if } (5) > V > (15) \\ 1, & \text{otherwise} \end{cases} \tag{3}$$

The parameters to compute f for R, G, and B channels are defined heuristically for each case, and they are shown in Fig. 5; the clustering of the shadowed and unshadowed regions is executed using a decision tree with different criteria for each mask, these differences are due to the different color characteristics for each channel ; the Fig. 5 displays the shadow detection factor calculation using a vertical decision tree block structure for R, G and B channels.

The parameters described at Fig. 5 are applied individually for each channel that is labeled in each row (red color, green color and blue color) in order to perform the shadow detection; Fig. 5 (a) defines the conditions when $\overline{x} < 100$, and

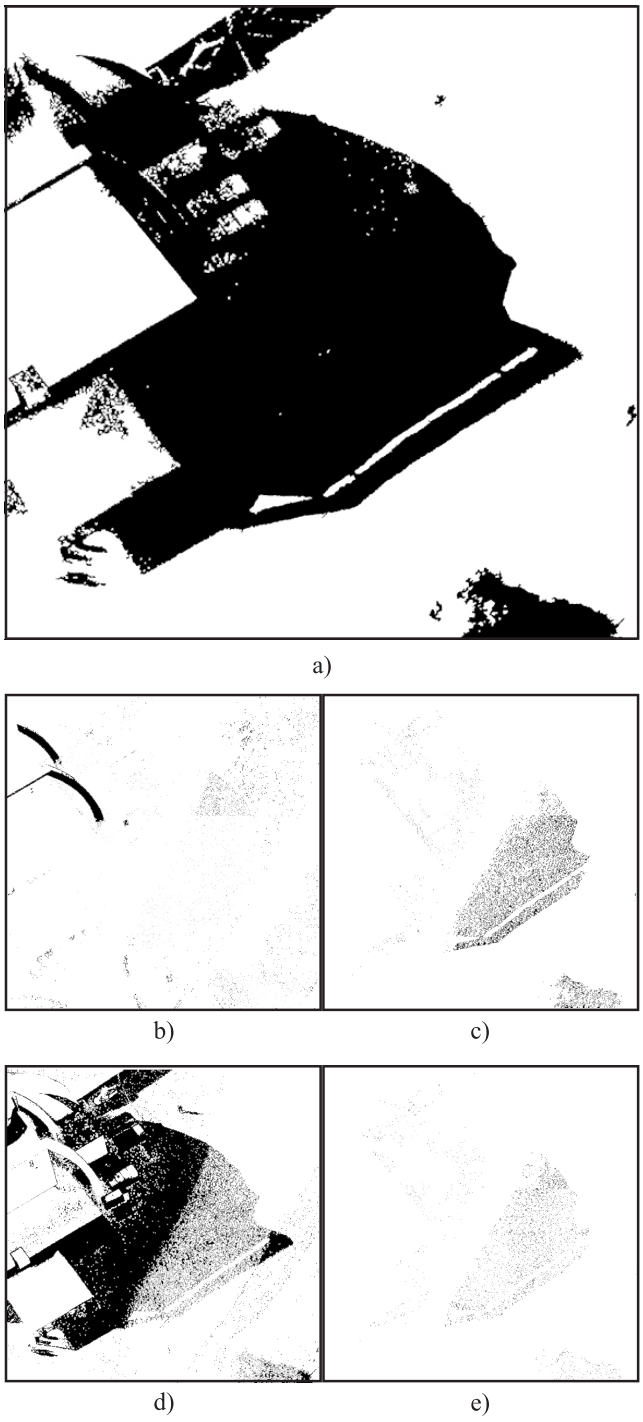

FIGURE 6. Shadow detection union (a), Shadow detection for channels R (b), G (c), B (d), and LS (e).

Fig. 5 (a) defines the conditions when $\bar{x} > 100$; the last step is to realize the union of shadow detection as shown in Fig. 6

IV. RESULTS AND DISCUSSION

The submitted method was tested using UAV captured images, in this case the mentioned images were captured with the previously described drone, the resolution of each picture is 3840 × 2880 pixels; it could be noticeable that the saturation and brightness of colors have a different behavior in their statistical distributions compared to satellite images, particularly, this difference is noticeable at image saturation values. The shadow color is not steady in this kind of images, where the texture of the regions is more noticeable in UAV images than in satellite images, and this can be noticed in the study cases shown in Fig. 7. In the case of Fig. 7 (a), the scenario includes urban regions, gardens and buildings, containing about 20% of shadowed zones that include all color zones; the sub-figure Fig. 7 (b) displays the shadow detection results (shadows are labeled in black) for the image described before. Sub-figure Fig. 7 (c) includes a scene that merely contains part of a freeway and green areas, in this image the shadows cover about of 75% of the image; the shadow detection result for this image described is shown in Fig. 7 (d). The third scenario is shown at Fig. 7 (e), which contains an urban region that contains green spaces, buildings, and asphalt with a shadow coverage taking near the 50% of the pixels; the shadow detection result is shown in Fig. 7 (f). Finally, the fourth image, which is shown at the sub-figure Fig. 7 (g), embeds an industrial zone take, where the shadows cover about the 40 % of the frame as it is shown at its shadow detection result at sub-figure Fig. 7 (h).

Furthermore, this proposal is also tested using satellite image of size 2000 × 2000 pixels, for which the sample images are shown in Fig. 8, such images are the same used by Silva *et al.* [25] shown in Fig. 8 (a) and (c), having Fig. 8 (e) and (g) as satellite images taken from the NY times [38], where it can be observed that the color characteristics regarding UAV camera pictures are different and as a result, the statistics might vary; the shadow detection results for each test is shown in Fig. 8 (b), (d), (f) and (h) respectively.

The proposed method is compared to the methodologies proposed by Silva *et al.* [25], Usha Nandini and Leni [28], Hosseinzadeh *et al.* [34], and the proposal presented by Suny and Mithila [35]. The main reasons behind this selection of methodologies for comparison purposes is the fact that the first two of them are applied using the intuitive color space characteristics to detect shadow regions by using two different approaches, and the second pair of methods include a machine learning algorithm and a CIELab color space method that works with the image luminance. The first methodology bases itself on using the Specthem ratio, the use of CIELCh color space and the Otsu's method of thresholding. Meanwhile, the second methodology uses K-means clustering and PSO for building its functionality. The third compared method is based on CNN, an Otsu's thresholding and a filtering process to segment shadows. Finally, the fourth method uses the L channel values to identify the amount of light in the regions of the image. The accuracy measurements are computed using rapid index (RI) and the results of this comparison is presented in Table 1, where, for shortness purposes, Silva *et al.* method is referenced as CIELCh-Otsu, Usha Nandini and Leni method is referenced

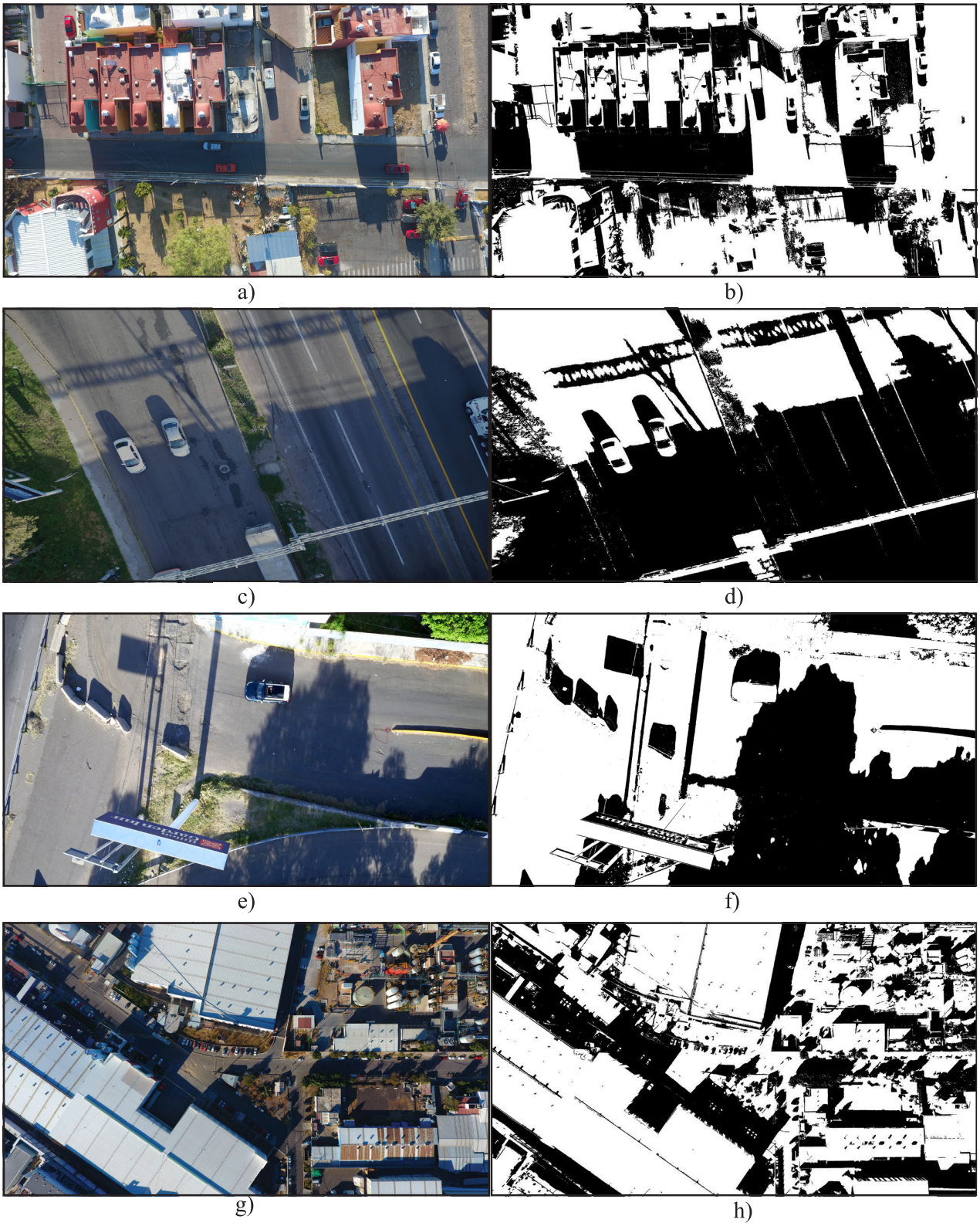

FIGURE 7. UAV captured images, a) image located in San Juan del Río, Qro (Test 1), b) shadow detection result for Test 1, c) image located in Querétaro City freeway (Test 2), d) shadow detection results for Test 2, e) image located in Querétaro city in urban zone (Test 3), f) shadow detection results for Test 3, g) image located in San Juan del Río, Qro in industrial zone (Test 4), and h) shadow detection results for Test 4.

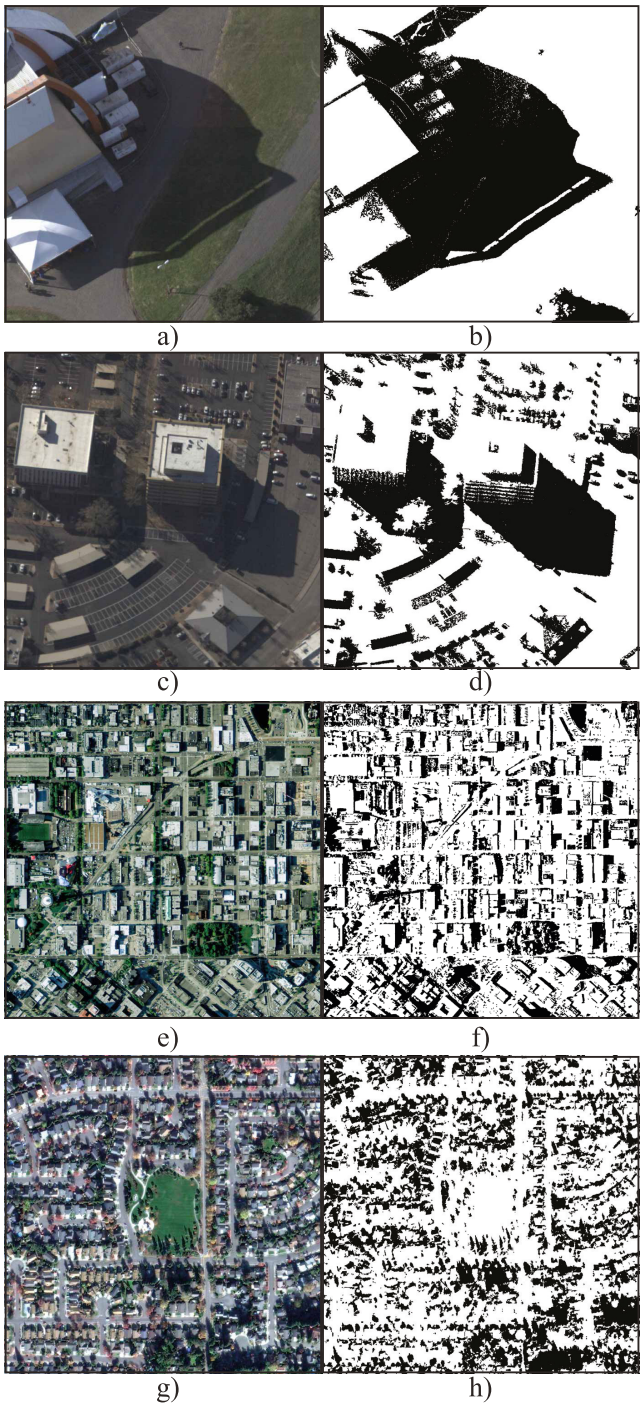

FIGURE 8. Satellite tested images, a) image acquired by the WAMI System in Porto Alegre, RS, Brazil (Test 1), b) shadow detection results for Test 1, c) image acquired by the WAMI System in Albuquerque, NM, US (Test 2), d) shadow detection results for Test 2, e) image taken form NY Times, South Lake Union, Seattle (Test 3), f) shadow detection results for Test 3, g) image taken form NY Times, Santa Rosa, California (Test 4), and h) shadow detection results for Test 4.

as PSO, Hosseinzadeh *et al.* method is referenced as CNN and Suny and Mithila method is referenced as CIELab.

As shown in Table 1, the proposed method obtained consistent RI results. Such outcome validates the accuracy of the proposal under different scenarios, showing this method as an ambivalent solution for satellite and UAV imagery. It is also evident the contrasts in results when satellite images are used compared to when UAV images are used, it is noticeable that results of the compared methods were affected when the mentioned image characteristics change. With the objective of carrying out further analysis of the results obtained, the under segmentation (US) and over-segmentation (OS) values are computed, where US is the proportion of the number of pixels, in which the shadowed regions were not detected, and OS indicates the rate of the number of unshadowed pixels that were miss-detected as shadows; where a higher value of OS or US denotes a higher rate of the described errors; the results for these features are shown in Table 2, where a comparison is performed against the same methodologies cited at the previous table.

TABLE 1. Statistics of each assessed RI for images from Fig. 7 and Fig. 8, comparing the proposed method, PSO, CNN, CIELab, and Otsu.

	Test	Proposed method	CIELCh-Otsu [25]	PSO [28]	CNN [34]	CIELab [35]
Satellite images	1	0.959	0.927	0.917	0.926	0.932
	2	0.922	0.925	0.890	0.922	0.921
	3	0.977	0.918	0.898	0.812	0.821
	4	0.987	0.931	0.892	0.749	0.877
UAV images	1	0.93	0.81	0.867	0.908	0.944
	2	0.942	0.855	0.515	0.604	0.892
	3	0.934	0.805	0.908	0.586	0.909
	4	0.971	0.871	0.827	0.743	0.793
AVG		0.953	0.880	0.839	0.781	0.886

As it can be observed, the proposed method presents accurate results in US and OS, the improvement of those values is more than 0.026 in US and more than 0.025 in OS for the compared methods, with higher differences in the results presented by the PSO methodology. In the case of the method based on CNN, it performs better at OS values, but at US values the values tend to increase for both kind of images, and it is noticeable that the CNN method loses accuracy in regions where the concrete and asphalt is dominant; finally, the CIELab color space based method tends to obtain consistent results, but it is dominated by the proposed method results in average. As it was previously stated, the methods tested against present higher US and OS results when the kind of images are changed from satellite images to UAV captured images as it could be seen at the partial average rows, this is mainly due to the characteristics of shadowed regions that are not the same in the satellite and UAV captured images. According to the results obtained for the testbench, the proposed method proved to be consistent at its results. The main advantage of the proposal is that the channel separation enables the individual analysis of color changes, also the addition of the LS channel enables detecting shadows in urban zone scenarios that include concrete and asphalt in an accurate way since the shadows in that kind of regions tends to change to blue color, with illuminated regions remaining on LS channel; last but not least, the channel separation procedure opens the possibility to change the shadow

TABLE 2. Statistics of each assessed US and OS for images from Fig. 7 and Fig. 8, comparing the proposed method, Otsu, PSO, CNN, and CIELab.

	Test	Proposed method		CIELCh-Otsu [25]		PSO [28]		CNN [34]		CIELab [35]	
		US	OS	US	OS	US	OS	US	OS	US	OS
Satellite images	1	0.025	0.016	0.032	0.041	0.062	0.021	0.066	0.008	0.054	0.013
	2	0.041	0.037	0.031	0.044	0.007	0.103	0.062	0.015	0.026	0.053
	3	0.009	0.001	0.012	0.069	0.05	0.044	0.182	0.007	0.178	0.004
	4	0.001	0.011	0.013	0.056	0.064	0.035	0.002	0.249	0.072	0.051
Satellite AVG		0.019	0.016	0.022	0.053	0.046	0.051	0.078	0.069	0.083	0.030
UAV images	1	0.039	0.025	0.117	0.069	0.1	0.027	0.073	0.013	0.014	0.036
	2	0.031	0.022	0.125	0.015	0.069	0.411	0.388	0.003	0.046	0.057
	3	0.007	0.001	0.140	0.007	0.017	0.026	0.365	0.001	0.006	0.037
	4	0.003	0.026	0.021	0.108	0.126	0.047	0.006	0.250	0.017	0.191
UAV AVG		0.020	0.019	0.101	0.030	0.049	0.128	0.208	0.066	0.021	0.080
AVG		0.020	0.018	0.062	0.042	0.048	0.105	0.089	0.068	0.052	0.055

detection parameters in only one channel without altering the results in the rest of channels.

V. CONCLUSION

The proposed approach was tested under different scenarios, where different scenes were as well as in different capturing devices at different illumination conditions: the selected images contained different characteristics that can present difficulties in the shadow detection process and its final results. According to the results obtained, the proposed method provided accurate results in an average of 8% over the other tested methods, this is especially noticeable in the UAV captured images, in which the other compared methods showed a less favorable behavior when analyzing the test images dataset, but in the case of the proposed approach the accuracy was consistent with no noticeable contrasts for both types of images.

The proposed channel separation workflow allowed performing the computing of statistical values for each one of them. This pipeline is useful due to the differences that every group of colors could present under different illumination conditions, and at the same time the shadowed urban regions that contain asphalt or concrete tends to be in the blue channel, whereas when unshadowed, its color is lowly saturated; this feature of the proposed methodology is mainly useful to detect those shadowed zones in the previously stated regions, it is also useful to keep good results when the type of picture changes. The channel separation is also helpful to analyze each channel shadows individually. This feature opens the possibility to improve the shadow detection in one channel without modifying the results in the rest of the channels, which could lead to more consistent developments to solve this task.

REFERENCES

[1] M. I. Elbakary and K. M. Iftekharuddin, "Shadow detection of man-made buildings in high-resolution panchromatic satellite images," *IEEE Trans. Geosci. Remote Sens.*, vol. 52, no. 9, pp. 5374–5386, Sep. 2014.

[2] Y. Zhao and B. Huang, "A two-step spatio-temporal satellite image fusion model for temporal changes of various lulc under one-pair prior images scenario," in *Proc. IEEE Int. Conf. Signal Process. Commun. Comput. (ICSPCC)*, 2016, pp. 1–5.

[3] A. Movia, A. Beinat, and F. Crosilla, "Shadow detection and removal in RGB VHR images for land use unsupervised classification," *ISPRS J. Photogramm. Remote Sens.*, vol. 119, pp. 485–495, Sep. 2016.

[4] G. Yan, L. Li, A. Coy, X. Mu, S. Chen, D. Xie, W. Zhang, Q. Shen, and H. Zhou, "Improving the estimation of fractional vegetation cover from UAV RGB imagery by colour unmixing," *ISPRS J. Photogramm. Remote Sens.*, vol. 158, pp. 23–34, Dec. 2019.

[5] H. O. Cruz, M. Eckert, J. M. Meneses, and J. F. Martinez, "Precise real-time detection of nonforested areas with UAVs," *IEEE Trans. Geosci. Remote Sens.*, vol. 55, no. 2, pp. 632–644, Feb. 2017.

[6] P. Radoglou-Grammatikis, P. Sarigiannidis, T. Lagkas, and I. Moscholios, "A compilation of UAV applications for precision agriculture," *Comput. Netw.*, vol. 172, May 2020, Art. no. 107148.

[7] B. U. Meinen and D. T. Robinson, "Mapping erosion and deposition in an agricultural landscape: Optimization of UAV image acquisition schemes for SfM-MVS," *Remote Sens. Environ.*, vol. 239, Mar. 2020, Art. no. 111666.

[8] Y. Lyu, G. Vosselman, G.-S. Xia, A. Yilmaz, and M. Y. Yang, "UAVid: A semantic segmentation dataset for UAV imagery," *ISPRS J. Photogramm. Remote Sens.*, vol. 165, pp. 108–119, Jul. 2020.

[9] X. Kang, Y. Huang, S. Li, H. Lin, and J. A. Benediktsson, "Extended random walker for shadow detection in very high resolution remote sensing images," *IEEE Trans. Geosci. Remote Sens.*, vol. 56, no. 2, pp. 867–876, Feb. 2018.

[10] W. D. Yang, W. Guo, K. Peng, and L. B. Liu, "Research on removing shadow in workpiece image based on homomorphic filtering," *Procedia Eng.*, vol. 29, pp. 2360–2364, Jan. 2012.

[11] H. Song, B. Huang, and K. Zhang, "Shadow detection and reconstruction in high-resolution satellite images via morphological filtering and example-based learning," *IEEE Trans. Geosci. Remote Sens.*, vol. 52, no. 5, pp. 2545–2554, May 2014.

[12] N. Tatar, M. Saadatseresht, H. Arefi, and A. Hadavand, "A robust object-based shadow detection method for cloud-free high resolution satellite images over urban areas and water bodies," *Adv. Space Res.*, vol. 61, no. 11, pp. 2787–2800, Jun. 2018.

[13] V. Gomes, P. Barcellos, and J. Scharcanski, "Stochastic shadow detection using a hypergraph partitioning approach," *Pattern Recognit.*, vol. 63, pp. 30–44, Mar. 2017.

[14] K. Higashi, S. Fukui, Y. Iwahori, Y. Adachi, and M. K. Bhuyan, "New feature for shadow detection by combination of two features robust to illumination changes," *Procedia Comput. Sci.*, vol. 96, pp. 896–903, Sep. 2016.

[15] K. R. M. Adeline, M. Chen, X. Briottet, S. K. Pang, and N. Paparoditis, "Shadow detection in very high spatial resolution aerial images: A comparative study," *ISPRS J. Photogramm. Remote Sens.*, vol. 80, pp. 21–38, Jun. 2013.

[16] Y. Wang, L. Wang, H. Lu, and Y. He, "Segmentation based rotated bounding boxes prediction and image synthesizing for object detection of high resolution aerial images," *Neurocomputing*, vol. 388, pp. 202–211, May 2020.

[17] M. Hammami, S. K. Jarraya, and H. Ben-Abdallah, "On line background modeling for moving object segmentation in dynamic scenes," *Multimedia Tools Appl.*, vol. 63, no. 3, pp. 899–926, Apr. 2013.

[18] M. Khare, R. K. Srivastava, and M. Jeon, "Shadow detection and removal for moving objects using Daubechies complex wavelet transform," *Multimedia Tools Appl.*, vol. 77, no. 2, pp. 2391–2421, Jan. 2018.
[19] S. Zhu, Z. Guo, and L. Ma, "Shadow removal with background difference method based on shadow position and edges attributes," *EURASIP J. Image Video Process.*, no. 22, pp. 1–15, 2012.
[20] C.-W. Lin, "Moving cast shadow detection using scale-relation multi-layer pooling features," *J. Vis. Commun. Image Represent.*, vol. 55, pp. 504–517, Aug. 2018.
[21] M. C. F. Macedo, V. P. Nascimento, and A. C. S. Souza, "Real-time shadow detection using multi-channel binarization and noise removal," *J. Real-Time Image Process.*, vol. 17, no. 3, pp. 479–492, Jun. 2020.
[22] S. H. Khan, M. Bennamoun, F. Sohel, and R. Togneri, "Automatic shadow detection and removal from a single image," *IEEE Trans. Pattern Anal. Mach. Intell.*, vol. 38, no. 3, pp. 431–446, Mar. 2016.
[23] G. Liasis and S. Stavrou, "Satellite images analysis for shadow detection and building height estimation," *ISPRS J. Photogramm. Remote Sens.*, vol. 119, pp. 437–450, Sep. 2016.
[24] V. J. D. Tsai, "A comparative study on shadow compensation of color aerial images in invariant color models," *IEEE Trans. Geosci. Remote Sens.*, vol. 44, no. 6, pp. 1661–1671, Jun. 2006.
[25] G. F. Silva, G. B. Carneiro, R. Doth, L. A. Amaral, and D. F. G. D. Azevedo, "Near real-time shadow detection and removal in aerial motion imagery application," *ISPRS J. Photogramm. Remote Sens.*, vol. 140, pp. 104–121, Jun. 2018.
[26] N. Mo, R. Zhu, L. Yan, and Z. Zhao, "Deshadowing of urban airborne imagery based on object-oriented automatic shadow detection and regional matching compensation," *IEEE J. Sel. Topics Appl. Earth Observ. Remote Sens.*, vol. 11, no. 2, pp. 585–605, Feb. 2018.
[27] S. Mohajerani and P. Saeedi, "Shadow detection in single RGB images using a context preserver convolutional neural network trained by multiple adversarial examples," *IEEE Trans. Image Process.*, vol. 28, no. 8, pp. 4117–4129, Aug. 2019.
[28] D. Usha Nandini and E. S. Leni, "Efficient shadow detection by using PSO segmentation and region-based boundary detection technique," *J. Supercomput.*, no. 75, pp. 3522–3533, 2018.
[29] D. Zhang, J. Han, G. Cheng, Z. Liu, S. Bu, and L. Guo, "Weakly supervised learning for target detection in remote sensing images," *IEEE Geosci. Remote Sens. Lett.*, vol. 12, no. 4, pp. 701–705, Apr. 2015.
[30] J. Nie, S. Qu, Y. Wei, L. Zhang, and L. Deng, "An infrared small target detection method based on multiscale local homogeneity measure," *Infr. Phys. Technol.*, vol. 90, pp. 186–194, May 2018.
[31] D. Zhang, J. Han, Y. Zhang, and D. Xu, "Synthesizing supervision for learning deep saliency network without human annotation," *IEEE Trans. Pattern Anal. Mach. Intell.*, vol. 42, no. 7, pp. 1755–1769, Jul. 2020.
[32] Y. Liu, Y. Wang, and A. W. K. Kong, "Pixel-wise ordinal classification for salient object grading," *Image Vis. Comput.*, vol. 106, Feb. 2021, Art. no. 104086.
[33] J. Tian, X. Qi, L. Qu, and Y. Tang, "New spectrum ratio properties and features for shadow detection," *Pattern Recognit.*, vol. 51, pp. 85–96, Mar. 2016.
[34] S. Hosseinzadeh, M. Shakeri, and H. Zhang, "Fastshadow detection from a single image using a patched convolutional neural network," in *Proc. IEEE/RSJ Int. Conf. Intell. Robots Syst. (IROS)*, 2018, pp. 3124–3129.
[35] A. H. Suny and N. H. Mithila, "A shadow detection and removal from a single image using lab color space," *Int. J. Comput. Sci. Issues*, vol. 10(4), no. 2, pp. 270–273, 2013.
[36] A. M. Polidorio, F. C. Flores, N. N. Imai, A. M. G. Tommaselli, and C. Franco, "Automatic shadow segmentation in aerial color images," in *Proc. 16th Brazilian Symp. Comput. Graph. Image Process. (SIBGRAPI)*, 2003, pp. 270–277.
[37] J. Huang, W. Xie, and L. Tang, "Detection of and compensation for shadows in colored urban aerial images," in *Proc. 5th World Congr. Intell. Control Automat.*, vol. 4, 2004, pp. 3098–3100.
[38] E. Badger and Q. Bui, "A decade of urban transformation, seen from above," *New York Times*, Dec. 2019.

GILBERTO ALVARADO-ROBLES received the B.E. degree in electromechanical engineering and the M.E. degree in mechatronics from the Autonomous University of Queretaro, Mexico, in 2013 and 2017, respectively, where he is currently pursuing the Ph.D. degree in engineering. His research interests include image processing, computer vision, and pattern recognition detection algorithms, mainly focused at analyzing images from satellite imagery and drones by using morphological operations.

ROQUE A. OSORNIO-RÍOS (Member, IEEE) received the Ph.D. degree in mechatronics from the Autonomous University of Queretaro, Queretaro, Mexico, in 2007. He is currently the Head Professor with the Autonomous University of Queretaro. He is a National Researcher level 3 with the Mexican Council of Science and Technology, CONACYT. He is an advisor for more than 80 theses. He has coauthored more than 90 technical papers published in international journals and conferences. His fields of interest include hardware signal processing and mechatronics. He is a Fellow of the Mexican Academy of Engineering. He is a part of the Editorial Board of the *Journal of Scientific and Industrial Research*.

FRANCISCO J. SOLÍS-MUÑOZ received the M.Sc. degree in computer engineering and mathematics from the Open University of Catalonia, Spain, in 2015. He is currently pursuing the Ph.D. degree in engineering with the Autonomous University of Queretaro, Mexico. He is specialized in the field of high-performance computing and algorithms with special interest on power quality monitoring solutions based on artificial intelligence techniques, smart cities, blockchain, and Industry 4.0. He received the Best Thesis Award in computer engineering and mathematics for his M.Sc. degree, which tackled the problem of task scheduling strategies for high-performance computing job queues. He is an Active Member of the Open Source Community.

LUIS ALBERTO MORALES-HERNÁNDEZ (Member, IEEE) received the degree in electromechanical engineering, the M.Sc. degree in instrumentation and automatic control, and the Ph.D. degree in engineering from the Faculty of Engineering, University Autonomous of Queretaro, Mexico, in 2004, 2005, and 2009, respectively. He is currently the Head Professor with the Faculty of Engineering, Autonomous University of Queretaro, where he also holds electromechanical engineering and mechatronics master's and Ph.D. positions, respectively. He is involved in some governmental projects and technology transfer contracts to industry. His research interests are in the fields of image processing, pattern recognition, and computer vision. He received the Best Thesis Award in engineering for his Ph.D. thesis.